# MODIFIED RATE EQUATION MODELS FOR UNDERSTANDING PERFORMANCE LIMITS OF VERTICAL AND IN-PLANE COMPOUND CAVITY VCSELS

**Naser F.G. Albugami[(a)], Eugene A. Avrutin[(b)],**

Dept of Electronic Engineering, University of York, Heslington, York YO10 5DD, UK

[(a)] na668@york.ac.uk, [(b)]eugene.arutin@york.ac.uk

## ABSTRACT

Modified rate equation models including both amplitude and phase properties are developed for advanced vertical cavity surface emitting lasers for multigigahertz modulation, and used to compare the performance of different designs and identify the corresponding limitations.

Keywords: vertical cavity laser, modified rate equation models, ultrafast modulation

## 1. INTRODUCTION

There are, fundamentally, two main approaches to increasing the modulation frequency range of vertical cavity semiconductor emitting lasers (VCSELs) at bit rates exceeding 40 GBit/s which can be used for high speed communication networks. The first one is through advanced developments in current (direct) modulation, which was demonstrated at bit rates up to 40 GBit/s (see e.g. Blokhin *et al.* 2009, Bobrov *et al.* 2015).

The second approach involves using some form of an advanced cavity structure. At least three solutions falling into the framework of this approach have been discussed. The first of them includes modulation of the photon lifetime in the passive cavity, rather than the curent (see e.g. Schchukin *et al.* 2014 and references therein) This approach promises substantially better dynamic properties than current modulation since it is free from the limitations of the direct modulation such as the the electron-photon resonance. The main laser design that alows this principle to be utilized is the copled-cavity VCSEL with one of the subcavities acting as an active one, and the other, as an electrooptic modulator (Van Eisden *et al.* 2008, Schchukin *et al.* 2008, Germann *et al.* 2012, Schchukin *et al.* 2014) or electroabsorption modulator (Chen et al. 2009) Modulation bit rates at least as good as those possible with direct modulation have been demonstrated in the references quoted, and rate equation analysis (Schchukin *et al.* 2008) predicts successful operation at bit rates up to and exceeding 80 GBit/s. However, rather than offering simple modulation of the photon lifetime, this design involves the laser oscillating in complex cavity modes, with the cavity decay time (photon lifetime), instantaneous frequency, and intensity all varying in time in a self-consistent way, which is not captured by rate equations and requires more sophisticated mathematical approaches.

A different type of an advanced cavity design involves using photon-photon resonance in some form, which comprises modulation of VCSEL arrays (Fryslie *et al.* 2015) and in-plane compound cavities, with amplified feedback from a slow wave waveguide resonator (see e.g. Dalir and Koyama 2011 and 2014, Park et al. 2016, and references therein).

A Lang-Kobayashi type delay-differential equation theory of the latter design has been presented in several papers (Dalir and Koyama 2011, Park et al. 2016), in the latter case with a good fit to the experiment achieved. This is despite of the fact that this model is, strictly speaking, intended for the case of weak optical feedback and as such used for the lasers in question (strong optical feedback) outside of its degree of applicability. The model was generalised to be more rigorous for the case of strong feedback, by introducing multiple delays, by Ahmed et al 2015, but the model is presented without derivation and appears to have a somewhat strange feature of the reflected light affecting he net gain rather than acting as an injected signal. Neither of the models includes the amplifying nature of the external feedback, it is not clear whether amplification in the feedback can help achieve further improvement in the laser performance. Finally, the question of what ultimately limits the laser performance does not appear to have been answered.

Thus, in order to understand the performance of both designs more accurately, and to compare those two approaches to improving the modulation properties, we have implemented a set of modified rate equation models each of which includes careful analysis of both amplitude and frequency (phase) of laser emission, as well as the spectrally selective nature of the laser cavity.


ISBN 978-88-97999-85-0; Affenzeller, Bruzzone, Jiménez, Longo and Piera Eds.

## 2. ELECTROOPTICALLY MODULATED LASER

### 2.1. The structure

Figure 1 shows the schematic of Cavity Laser which we used in our analysis. The laser is formed by two sub-cavities. The top, modulator, sub-cavity is a passive Fabry-Perot resonator whose reflectivity $R_m(t)$ is modulated via electro-optically varying the optical properties of a modulator layer contained within the sub-cavity by applying time-varying reverse bias voltage. In a typical design, the intermediate DBR has 25-35 periods of two layers of alternating composition, the top DBR consists of 15-25 periods; the resonator thus can be substantially asymmetric. Throughout the analysis, we consider only refractive index modulation (no absorption modulation). Indeed, it has been shown in the literature (see e.g. Schchukin *et al.* 2008) that in a practical design of this type, the electrorefraction effect plays a dominant role in modulating $R_m(t)$ as compared to electroabsorption.

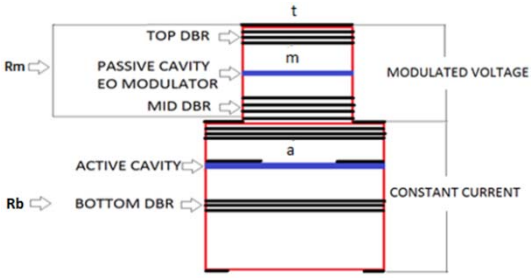


Figure 1: Schematic of a Compound Cavity Laser and model setup

### 2.2. The model

In designing the model (Albugami and Avrutin 2017), we follow the approach used previously for Distributed Feedback (DFB) lasers ( see e.g. Wenzel *et al.*, 1996 ) and for multimode compound cavity lasers ( see e.g. Avrutin *et al.*, 1999). Namely, the laser cavity is treated as a complex resonator, and a complex eigenfrequency of this resonator is found, which is then used to describe the laser dynamics. The electrooptically modulated VCSEL is very naturally suited for such an approach, because the complex resonator in this case can be defined by considering the active sub-cavity as a quasi-Fabry-Perot resonator terminated, on one side, by the bottom reflector with a (complex, generally speaking) amplitude reflectance $r_b$ and on the other side, by the EO modulator subcavity treated as a passive, frequency-dependent reflector with a complex reflectance $r_m(\omega)$, where $\omega$ is the complex eigenfrequency sought. The value of the modulator reflectance is calculated from the equation

$$R_m = r_m r_m^* \quad (1)$$

$$r_m = r_{am} + \frac{\rho_{am}\,\rho_{ma}\,r_{mt}\,e^{-j2K_m L_m}}{1 - r_{ma}\,r_{mt}\,e^{-j2K_m L_m}}$$

with the average wave vector in the form of:

$$K_m(\omega) = \frac{(n_m + \Gamma^t_m \Delta n_{EO})\omega}{c} \quad (2)$$

Here, $\Delta n_{EO}$ describes the time-dependent correction to the refractive index of the modulator layer caused by electrooptic modulation. $\Gamma^t_m \approx \frac{d_m}{L_m}$ (assuming the modulator layer is thick enough that the standing wave factor is near one) is the confinement factor of the modulator layer, $d_m$ being the modulator layer thickness and $L_m$, the total physical thickness of the modulator cavity, including any spacer layers between the modulator layer and the reflecting stacks but not including the penetration into mirrors. The complex eigenfrequency is then found by solving the usual threshold/resonant condition of a Fabry-Perot type cavity (the short cavity length ensures that the equation has one solution):

$$r_m(\omega)\, r_b(\omega) \times \exp\left[2\left(-j\frac{(n_a + \Delta n_a)\omega}{c} + \Gamma^t_a \frac{g}{2}\right)L_a\right] = 1 \quad (1)$$

It is convenient to write the solution to this equation in terms of a frequency correction $\Delta\omega = \omega - \omega_{ref}$, where the (real) reference frequency $\omega_{ref}$ is arbitrary but can be conveniently taken, for example, as the position of the reflectance spectrum notch (**Errore. L'origine riferimento non è stata trovata.**) in either on or off-state. Then, the complex instantaneous frequency correction $\Delta\omega$ is given by a transcendental equation:

$$\Delta\omega = v_g \left[-\frac{I}{2}\left(\Gamma^t_a g - \frac{1}{L_a}\ln\frac{1}{r_m(\omega_{ref}+\Delta\omega)r_b}\right) - \frac{\Delta n_a\,\omega_{ref}}{c} + \left(\frac{q\pi}{L_a} - \frac{n_a\,\omega_{ref}}{c}\right)\right] \quad (2)$$

Here, $v_g$ is the group velocity, $L_a$ is the geometrical thickness of the active subcavity, $\Gamma^t_a$ is the confinement factor for the active area, $g$ is the time-dependent gain, $n_a$ is the refractive index of the active layer subcavity, averaged over the length in the same way as $n_m$ is averaged over the modulator subcavity. The refractive index varies in time primarily due to self-phase modulation in the active layer; its time-dependent part can be quantified as:

$$\Delta n_a \approx \frac{c}{2\omega_{ref}}\Gamma^t_a \alpha_H (g - g_{th}) \quad (5)$$

where $\alpha_H$ is the Henry linewidth enhancement factor in the active layer and $g_{th}$ is the gain at threshold which we used as a reference value.


ISBN 978-88-97999-85-0; Affenzeller, Bruzzone, Jiménez, Longo and Piera Eds.

The choice of reference frequency near the modal frequency to ensure that $|\Delta\omega| \ll \omega_{ref}$ means that we can introduce a parameter $q$ which is the number of half-wavelengths of light in material fitting (roughly) in the distance $L_a$. It depends on the VCSEL design, mainly the thickness $L_a$, and it is an integer number chosen in such a way that

$$q \approx \frac{2n_a L_a}{\lambda} - \frac{1}{2\pi}\arg(r_m r_t) \quad (6)$$

where $\lambda=2\pi c/\omega_{ref}$ is the operating wavelength, and $r_m$ can be estimated in the on- or off-state.

The frequency ω (or frequency correction Δω) has a real part, which determines the time-dependent spectral position of the lasing mode and thus the chirp of laser emission, and an imaginary part, which reflects the balance of gain and loss (the latter including the outcoupling loss, which is frequency dependent through $r_m(\omega)$). The imaginary part determines the dynamics of photon density (in the active cavity) $N_p$, giving a modified rate equation in the form:

$$\frac{dN_p}{dt} = -2 * \mathrm{Im}(\Delta\omega(t))N_p(t) + \frac{\beta_{sp}N}{\tau_{sp}(N)} \quad (7)$$

Where $\tau_{sp}$ is the carrier spontaneous recombination time and $\beta_{sp}$ is the spontaneous emission factor. The dynamics of the carrier density $N$ is determined by a standard rate equation:

$$\frac{dN}{dt} = \frac{\eta_i I}{eV} - \left(\frac{1}{\tau_{sp}(N)} + \frac{1}{\tau_{nr}(N)}\right)N - v_g \frac{g(N)}{1+\varepsilon N_p} \quad (4)$$

in which $N$ and $N_p$ are the the electron and photon densities, respectively, $\eta_i$ is the internal quantum efficiency, $I$ is the injected current, $e$ is electron charge, $V$ is the volume of the active region; $\tau_{sp} = [B_1 N^2/(1+b_1 N)]^{-1}$ and $\tau_{nr} = (A_1 + C_1 N^2)^{-1}$ are the spontaneous and nonradiative recombination times of carriers, respectively, $g(N)$ is the optical gain in the active layer, $\varepsilon$ is gain compression factor (see Table 1).

Finally, the model includes a differential equation taking into account the electromagnetic resonance in the modulator cavity. The equation is derived by considering the modulator section in frequency domain and then substituting the imaginary part of the frequency correction by a time derivative. The result is conveniently expressed as:

$$\frac{d\tilde{E}_t}{dt} = \frac{\sqrt{1-R_t}}{4}\frac{v_g}{L_{eff,m}}\tilde{E}_a + \left(-\frac{1}{2\tau_{cm}} - j\left(\Delta\omega'(t) - \Delta\omega_{n0} + \Gamma_m \frac{\alpha_{int}(\tau)}{n_g}\omega_{ref}\right)\right)\tilde{E}_t \quad (9)$$

$$\tau_{cm} = \frac{L_{eff,m}}{v_g(1-\sqrt{R_t R_b})} \approx \frac{2L_{eff,m}}{v_g(T_t - T_t)} \quad (10)$$

Here, $\tilde{E}_t = E_t \exp(j\varphi_t)$ describes the complex amplitude of the output field emitted from the modulator subcavity (the top mirror), $E_a = \sqrt{N_p}$ is the field amplitude inside the active subcavity. Note that in the equation written in the form above, $E_a$ is a *real* value, which means that the complex amplitude of the output light is actually $\tilde{E}_t^{out} = \tilde{E}_t \exp(j\int \Delta\omega' dt)$, where $\Delta\omega'=\mathrm{Re}(\Delta\omega)$ is the instantaneous frequency correction in the active cavity. Furthermore, $\Delta\omega_{n0}=\omega_{n0}-\omega_{ref}$ is the position of the notch in the modulator subcavity transmission in the absence of modulation ($\Delta_{nEO} = 0$), $\tau_{cm}$ is he effective photon lifetime in the modulator cavity, $R_t = |r_{int}|^2$ and $R_t = |r_{int}|^2$ are the intensity reflectances of the intermediate and top reflectors (the two reflectors forming the modulator cavity) respectively, $T_t = 1 - R_t$, $T_t = 1 - R_t$ are the transparencies of the intermediate and top DBR stacks, and $L_{eff,m}$ is the effective thickness of the modulator section; it is typically a fraction of a micrometer greater than the physical one, as it considers the penetration of the field into the mirrors. The power emitted from the laser can be calculated as:

$$P \approx v_g \hbar\omega A_x E_t^2 \quad (11)$$

Where $A_x$ is the cross-section of the aperture

An alternative formalism for describing the laser dynamics with phase included would consist of writing out an equation similar to equation (**Errore. L'origine riferimento non è stata trovata.**) for the *active* subcavity, with an injection term representing light reflected from the modulator cavity, rather than solving a transcendental equation (**Errore. L'origine riferimento non è stata trovata.**) for the instantaneous frequency. A model of that type twould the laser as a system of two subcavities, one active, one passive but modulated, treated on the same footing. The results should be very similar to those of the current formalism so long as the dynamics of light *inside* the active cavity remain slower than the modulator cavity round-trip (which is the case for most realistic designs).

### 2.3. Small-signal analysis

The small-signal analysis was performed analyticallyAlbugami and Avrutin 2017. Typical results are shown in Figure 2.

The figure illustrates that the ultimate limit to the modulation speed is set by the photon lifetime in the modulator section, which in turn is determined by the reflectances of the top and intermediate reflectors. With the optimised laser design (a large $R_i$ ensuring the external-modulator-type operation of the modulator section, and a more modest $R_t$ ensuring the value of $\tau_{cm}$ of the order of picoseconds), this limit is of the order of hundreds of gigahertz, and thus not a concern for any realistic modulation scheme.


ISBN 978-88-97999-85-0; Affenzeller, Bruzzone, Jiménez, Longo and Piera Eds.

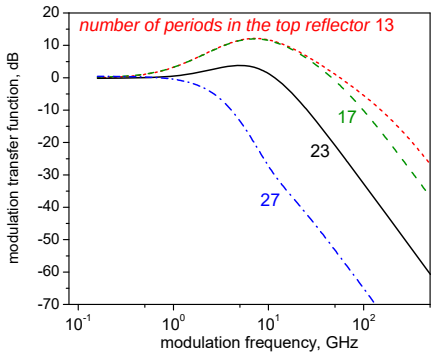


Figure 2. Calculated small-signal response of EO laser modulation. 35 periods in the intermediate reflector

The situation can be different however with a design of the modulator section less optimised for high speed operation. With a large (but perfectly technologically achievable) number of periods in the top reflector (hence $R_t$), when the notch in the reflectance of the modulator section (the peak in the transmittance) becomes narrow meaning a large photon lifetime in the modulator cavity, the 3dB frequency drops as low as ~10 GHz. As will be discussed later, these effects of the reflector design manifest themselves also in the results of *large* signal modulation simulationsLarge signal analysis

### 2.4. Large- signal analysis

The large signal analysis was implemented as a Matlab code; the transcendental equation (4) was solved at each step using the direct iteration method and with the value at the previous point in time used as the initial condition; typically only 3-4 iterations were required.

The large signal modulation laser behaviour was characterized using an eye diagrams (Figures 3-4) and quantified additionally by means of a Quality Factor

$$Q = \frac{\overline{P_{(1)}} - \overline{P_{(0)}}}{\sigma_{(1)} + \sigma_{(0)}} \qquad (11)$$

where $\overline{P_{(1)}}$, $\overline{P_{(0)}}$ are the mean values of the power corresponding to the logical one and zero states, respectively; $\sigma_{(1)}$, $\sigma_{(0)}$ are the corresponding standard deviations.

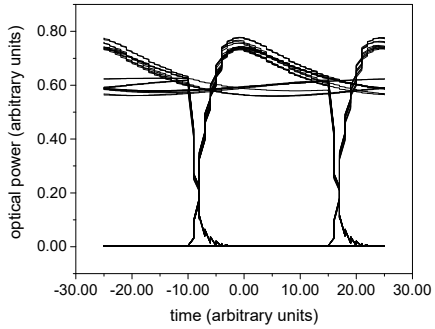


Figure 3. Eye diagrams for $i$= 10 mA, 40 GBit/s, 35 intermediate DBR periods, 17 top DBR periods

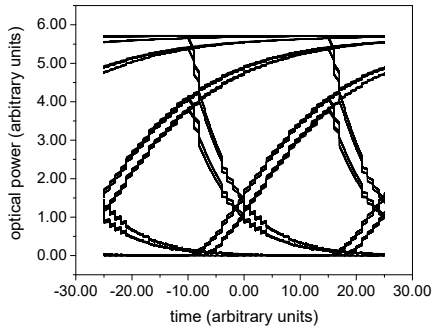


Figure 4. As figure 3, 23 top DBR periods

Figure 5 shows Q as function of the number of layer pairs (periods) in the *top* reflector DBR stack. As seen in the figure, there is an optimum number, in this case around 17.

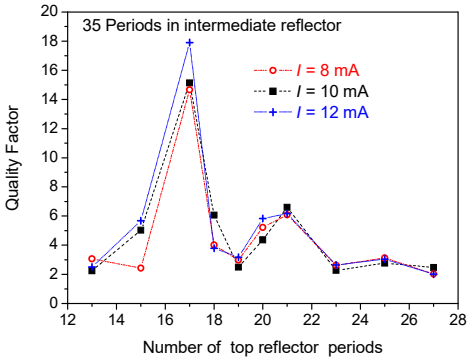


Figure 5: Modulation quality factor as function of the number of periods in the top reflector

When we increase the number of periods beyond that number, the photon lifetime in the modulator cavity is increased, leading to longer transients and closing the eye diagram, hence bad quality factor. When the number of top reflector period becomes too low, on the other hand, the power variation ($P_1$-$P_0$) becomes lower, hence lower quality factor. We observe that the optimum number of periods is not a strong function of

the current, so once optimised, a laser should be able to provide good modulation quality at all currents.

Figure 6. shows the modulation quality as a function of the number of periods in the *intermediate* reflector. Again, there is an optimum number of periods, in this case around 32.

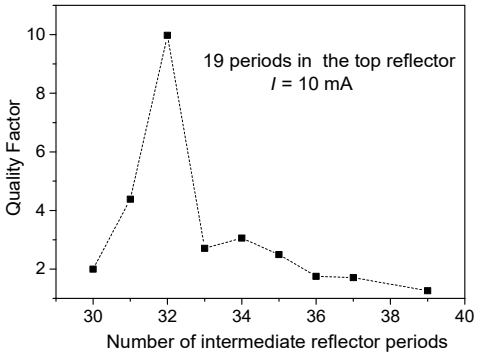


Figure 6: Modulation quality factor as function of the number of periods in the intermediate reflector Bit rate 40 GBit/s

An advantage of the electrooptic modulation is the relatively low chirp predicted. Despite a certain degree of phase modulation implied by Eqs, 4 and 7 (the phase and amplitude of the modulator reflectance are by necessity modulated simultaneously), the spectra of laser emission simulated (Figure 7) are almost transform limited.

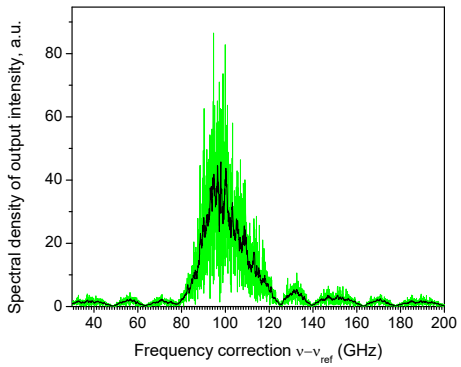


Figure 7: Amplitude Spectrum of output Field at 40 GBit/s

## 3. LASER WITH IN-PLANE FEEDBACK

In the first part of the work, we used a heuristic Lang-Kobayashi model similar to that used by Dalir and Koyama 2011 and adopted by some other authors (e.g. Park et al. 2016), with the rate equation for the electric field inside the cavity given by the rate equation with the delayed term:

$$\frac{dE(t)}{dt} = G^{net}(t)E(t) + KE(t-\tau_c) \qquad (12)$$

Where the spontaneous term has been omitted (it was introduced in simulations using a Langevin noise source but omitted for small-signal simulations),

$$G^{net}(t) \approx \frac{1}{2}\left[v_g\Gamma g(1+j\alpha_H) - \left(\frac{1}{\tau_{ph}^{z}} + \frac{1}{\tau_{ph}^{xy}} + \frac{1}{\tau_{ph}^{in}}\right)\right] \qquad (13)$$

is the complex amplitude net gain, with the photon lifetime including contributions due to the vertical cavity, in-plane cavity, and internal losses; the rest of parameters have the same meaning as for the vertical cavity.

Finally, $K$ is the heuristic optical feedback coefficient (in the case of a one-dimensional cavity with small feedback, it can be expressed in terms of (ii) the coupling between the laser and the external cavity and (ii) the reflectance of the distant reflector). The coefficient is complex, with its phase having a large effect on the laser dynamics.

When analysing the small-signal response, we use the impulse response method, applying a short (~2-5 ps) Gaussian current pulse to the laser and taking a Fourier transform of the resulting transient. This allows to make an express estimate of the 3dB cutoff frequency.

Typical results are shown in Figure 8. As in previous results, in-phase feedback increases the frequency of the relaxation oscillations and hence the 3dB modulation cutoff; however the limit to utilising this frequency increase by increasing the feedback is set by the onset of self-pulsations, with the relaxation oscillations becoming undamped.

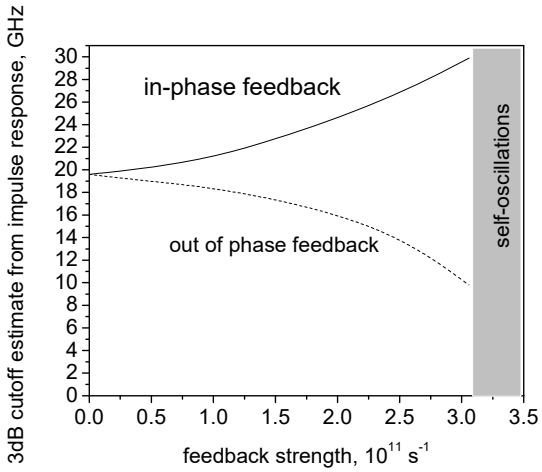


Figure 8. Estimate for 3dB modulation bandwidth using the impulse response method in the Lang-Kobayashi type model.


ISBN 978-88-97999-85-0; Affenzeller, Bruzzone, Jiménez, Longo and Piera Eds.

Including amplification in the external cavity by making the coefficient $K$ time-dependent according to the model by Antonelli et al. 2015 does not appear to modify the result qualitatively.

Next, we attempted to extend the analysis from the heuristic approach of Dalir and Koyama 2011, based on Lang Kobayashi equations with a single delay, to a more electromagnetically justified model. In doing so, the complication is that we cannot restrict ourselves even approximately to one-dimensional analysis as in the vertical cavity problem, as the in-plane cavity problem is substantially multi-dimensional. In the case of a cavity with rectangular geometry as used by Park et al. 2016, we can restrict the analysis to two dimensions: the vertical dimension z and the direction of the in-plane cavity $x$, as shown in Figure 9 (in the third dimension $y$, the lateral one perpendicular to the external cavity orientation, a well-localised single lateral mode is assumed).

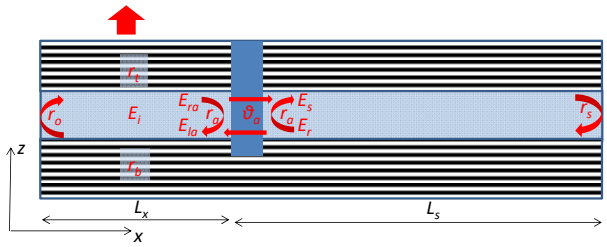


Figure 9: Schematic of the electromagnetic 2D model for a compound in-plane cavity.

In the in-plane direction, the laser is just a section of the slow-wave waveguide, of a length $L_x$, with gain due to the amplification in the active layer and loss due to both internal loss and emission through the top and bottom mirrors. The section is terminated on the left hand side by the outer reflectance $r_o$ (typically $|r_o|\sim 1$), and on the right, by an oxide stripe separating the laser from the amplifier (slow waveguide external cavity). The oxide stripe is assigned an amplitude reflectance $r_a$ and an amplitude transmittance $\sqrt{\vartheta_a}\exp(j\varphi_\vartheta)$, $\vartheta_a$ being the intensity transmittance and $R_a = |r_a|^2$ the intensity reflectance. If there is no scattering of light out of the slow-waveguide mode in the oxide, $R_a + \vartheta_a = 1$; in reality it is likely that some scattering is present so $R_a + \vartheta_a < 1$. In the analysis, we assumed that the reflectance $r_a$ is seen by the light travelling in both directions. It has to be pointed out that this applies better to the linear geometry cavity of Park et al. 2016, than to the more three-dimensional geometry of Dalir and Koyama 2014, in which the waveguide connecting the external and laser cavities is narrow, and the oxide reflectance is not necessary for determining the mode of the laser cavity.

In the model considered, the dynamic equation for the light amplitude inside the cavity takes the form

$$\frac{dE_i}{dt} = \frac{1}{\tau_x e^{g_{max}\tau_x}}\left\{\sqrt{f_x\vartheta_a}\, e^{j\varphi_\vartheta} E_r + \left(e^{g_{max}\tau_x} - 1\right) E_i\right\} \quad (14)$$

Here, $T_x$ is the round-trip of the slow wave along the laser size $L_x$, and f is the geometric factor (~2 in a good quality cavity). The reflected light amplitude $E_r$ in the passive external cavity limit is given by

$$E_r(t) = r_s E_s(t - \tau_s) \quad (15)$$

Where $r_s = |r_s|\exp(j\varphi_s)$ is the field reflectance of the remote reflector (Figure 8), and

$$E_s(t) = \sqrt{\frac{\vartheta_a}{f_x}} e^{j\varphi_\vartheta} \frac{1}{\tau_a} e^{g_{max}\tau_x} E_i(t) + r_a E_r(t) \quad (16)$$

is the field to the right of the oxide stripe travelling into the external cavity. The "recursive" boundary conditions (15-16) eliminate the need for summing the terms from multiple delays which needs to be done in the model by Ahmed et al. 2015, and also allow for the gain in the external cavity to be included along the lines of the paper by Antonelli et al. 2015. In the limit of weak external reflectance, the second term in (16) disappears, and the model reduces to the Lang-Kobayashi type one.

The results of the model, while quantitatively different from those of the Lang Kobayashi type model, predict a similar increase in the modulation frequency cutoff of the order of the frequency itself, in other words up to the values of 30-40 GHz but, at least in our simulations so far, not beyond.

## 4. CONCLUSIONS.

We have presented the two modified rate equations approaches suitable for analysis of advanced ultrafast lasers: the compound-cavity eigenmode model for the vertically integrated electrooptically modulated laser and a delay-differential one for the laser with in-plane compound cavity.

In terms of sheer modulation potential, the electrooptically modulated laser appears to be the more promising, with modulation cutoffs determined ultimately by the photon lifetime in the external cavity and thus, with proper design, extending into hundreds of gigahertz.

Practical considerations such as the ease and cost of fabrication and integration, ambient temperature tolerance, etc. will also contribute to determining the laser design to be used in each particular application.


ISBN 978-88-97999-85-0; Affenzeller, Bruzzone, Jiménez, Longo and Piera Eds.

**REFERENCES**


Ahmed, M., Bakry, A., Alghamdi, M. S., Dalir, H. & Koyama, F, 2015. Enhancing the modulation andwidth of VCSELs to the millimeterwaveband using strong transverse slow-light feedback. *Opt. Express* **23,** 15365

Antonelli C., Mecozzi A., Hu Z., Santagiustina M., 2015. Analytic study of the modulation response of reflective semiconductor optical amplifiers, J.Lightwave Technol., 22(20), 4367-4376

Albugami N.F. and Avrutin E.A. 2017, Dynamic modelling of electrooptically modulated vertical compound cavity surface emitting semiconductor lasers, Opt.Quantum Electron., accepted.

Avrutin, E.A., Marsh, J.H., Arnold, J.M., Krauss, T.F., Pottinger, H., De La Rue, R.M. 1999. Analysis of harmonic (sub)THz passive mode-locking in monolithic compound cavity Fabry-Perot and ring laser diodes. IEE Proc. Optoelectron. 146(1), 55–61

Blokhin, S.A., Lott, J.A., Mutig, A., Fiol, G., Ledentsov, N.N., aximov, M.V., Bimberg, D., 2009. Oxide confined 850 nm VCSELs operating at bit rates up to 40 Gbit/s. Electron. Lett. 45(10), 501–502

Bobrov, M.A., Blokhin, S.A., Maleev, N.A., Kuzmenkov, A.G., Blokhin, A.A., Yu, M.Z., Ustinov, V.M., 2015. Ultimate modulation bandwidth of 850 nm oxide-confined vertical-cavity surface-emitting lasers. J. Phys: Conf. Ser. 643(1), 012044

Chen C., Leisher P.O., Grasso D.M., Long C., Choquette K.D. 2009, High-speed electroabsorption modulation of composite-resonator vertical cavity lasers, IET Optoelectronics, 3(2), 93-99

Dalir, H. and Koyama F., 2011. Bandwidth enhancement of single-mode VCSEL with lateral optical feedback of slow light. IEICE Electronics Express, 2011. **8**(13), 1075-1081

Dalir, H. and Koyama F., 2014, Highly stable operations of transverse coupled cavity VCSELs with enhanced modulation bandwidth, Electron.Lett., 50 (11), 823-824

Fryslie S.T.M., Tan M.P., Siriani D.F., Johnson M.T., and Choquette K.D. 2014 . 37-GHz modulation via resonance tuning in single-mode coherent vertical-cavity laser arrays. IEEE Photon. Technol. Lett. 27(3), 415–418

Germann TD, H.W., Nadtochiy AM, Schulze JH, Mutig A, Strittmatter A, Bimberg D., 2012. Electro-optical resonance modulation of vertical-cavity surface-emitting lasers. Opt Express, **20**(5), 5099-107

Park, G.C., Xue, W., Piels, M., Zibar, D, Mork, J, Semenova, E., Chung, I-S, 2016. Ultrahigh-speed Si-integrated on-chip laser with tailored dynamic characteristics, Scientific Reports, 6, 38801.

Shchukin, V.A., Ledentsov, N.N., Lott, J.A., Quast, H., Hopfer, F., Karachinsky, L.Y., Bimberg, D. 2008. Ultrahigh-speed electro-optically modulated VCSELs: modeling and experimental results. Proc. SPIE 6889(1), 68890H .

Shchukin, V.A., Ledentsov, N.N., Qureshi, Z., Ingham, J.D., Penty, R.V., White, I.H., Novikov, I.I. 2014. Digital data transmission using electro-optically modulated vertical-cavity surface-emitting laser with saturable absorber, Appl. Phys. Lett. 104(5), 051125

Van Eisden J., Yakimov M, Tokranov V., Varanasi M., Mohammed E. M., Young I. A., Oktyabrsky S. R. 2008, Optically Decoupled Loss Modulation in a Duo-Cavity VCSEL, Photon.Technol. Lett., 20(1),42-44

Wenzel, H., Bandelow, U., Wunsche, H.J., Rehberg, J. 1996, Mechanisms of fast self pulsations in two-section DFB lasers. IEEE J. Quantum Electron. 32(1), 69–78